Journal of Molecular Catalysis A: Chemical 411 (2016) 1–11

Contents lists available at ScienceDirect

Journal of Molecular Catalysis A: Chemical

journal homepage: www.elsevier.com/locate/molcata

Partial oxidation of ethanol on supported Rh catalysts: Effect of the oxide support

Mariann Tóth, Erika Varga, Albert Oszkó, Kornélia Baán, János Kiss*, András Erdőhelyi

Department of Physical Chemistry and Materials Science at the University of Szeged, Aradi vértanúk tere 1, H-6720 Szeged, Hungary

ARTICLE INFO

Article history:
Received 31 July 2015
Received in revised form
11 November 2015
Accepted 12 November 2015

Keywords:
Partial oxidation of ethanol
Rh/Al_2O_3 catalyst
Rh/SiO_2 catalyst
Rh/TiO_2 catalyst
Rh/CeO_2 catalyst

ABSTRACT

In this work, the effect of the nature of oxide support on the reaction mechanism of the partial oxidation of ethanol on Rh catalyst was studied by diffuse reflectance infrared (DRIFTS) and X-ray photoelectron spectroscopy (XPS). The conversion of ethanol and the product distribution were analysed by gas chromatography. The highest ethanol conversion was measured on Rh/CeO_2 catalyst. The results showed that the nature of the oxide support affected the reaction mechanism. On supported Rh catalysts ethanol adsorption gives rise to ethoxide species, which can be decomposed to CO_2, CO and CH_4 and dehydrogenated, forming acetaldehyde. The latter species are oxidized to acetate or dehydrogenated to acetyl species on Rh/Al_2O_3 and on Rh/CeO_2. On Rh/TiO_2 the acetaldehyde can also be oxidized in a parallel process to $HCOOH/HCOO_{(a)}$ which forms CO_2 and water. Furthermore, the acetate species previously formed can be decomposed to CH_4, CO and/or oxidized to CO_2 via carbonate species at higher temperature depending on the oxide support. On silica support acetaldehyde was the dominant intermediate and it desorbed or directly decomposed with or without oxygen to CO_2 and methane. The partial oxidation of ethanol proceeds on partially oxidized Rh sites on Rh/Al_2O_3, Rh/TiO_2 and on Rh/CeO_2. In spite of the presence of O_2, ceria is not fully oxidized during the partial oxidation of ethanol.

1. Introduction

Alcohol oxidation reactions are used in industrial processes for energy conversion and as starting materials for the synthesis of organic chemicals and pharmaceuticals. For example, several highly effective fuel cell types are based on the complete oxidation of low molecular weight alcohols [1,2], while complex alcohols are used in the production of drugs and fine chemicals [3,4]. There are numerous studies focusing on the catalytic oxidation of ethanol with molecular oxygen. Usually liquid phase reactions are performed at near-ambient temperatures [5], while elevated temperatures are used for gas phase alcohol oxidation [6–9]. Ethanol has great advantage over other fuels; it can be produced directly by the fermentation of bio-mass so it is an environmentally friendly material.

In order to understand the different ethanol transformation processes including steam reforming (SRE) and oxidative steam reforming (OSRE) of ethanol, it is worth investigating deeply ethanol oxidation on metal supported oxide catalysts.

In the course of the full oxidation of ethanol carbon dioxide and water are formed:

$$C_2H_5OH + 3O_2 \rightarrow 2CO_2 + 3H_2O \ \Delta H = -1277\,kJ\,mol^{-1} \quad (1)$$

Naturally, for different applications the partial oxidation routes of ethanol (POX) could be more interesting. Unlike partial oxidation of hydrocarbons, that of ethanol is slightly endothermic:

$$C_2H_5OH + 1.5O_2 \rightarrow 2CO_2 + 3H_2 \ \Delta H = 510\,kJ\,mol^{-1} \quad (2)$$

$$C_2H_5OH + 0.5O_2 \rightarrow 2CO + 3H_2 \ \Delta H = 14\,kJ\,mol^{-1} \quad (3)$$

$$C_2H_5OH + 0.5O_2 \rightarrow CH_3CHO + H_2O \ \Delta H = -173\,kJ\,mol^{-1} \quad (4)$$

The pathways depend on the reaction conditions such as reaction temperature, ratio of reactants, space velocity and mainly on the nature of the catalytic system including the active components and type of support. The reforming of ethanol is an endothermic reaction but by mixing oxygen to water the process became autothermic (oxidative steam reforming):

$$C_2H_5OH + 2H_2O + 0.5O_2 \rightarrow 2CO_2 + 5H_2 \ \Delta H = -68\,kJ\,mol^{-1} \quad (5)$$

From this respect the study of partial oxidation of ethanol offers useful data for understanding the oxidative steam reforming process (OSRE).

The partial oxidation of ethanol has been studied over a series of silica supported noble metal catalysts [10]. Pt was found to be the

* Corresponding author. Fax: +36 62 420 678.
E-mail address: jkiss@chem.u-szeged.hu (J. Kiss).

http://dx.doi.org/10.1016/j.molcata.2015.11.010
1381-1169/

most active for the formation of CO_2 and Ru was highly selective for the formation of acetaldehyde below 373 K. CeO_2 supported Ni was also active in acetaldehyde formation while on Pt/CeO_2 methane was produced [11]. On this Pt/CeO_2 sample at low temperature also acetaldehyde was the main product, but at higher temperature when the CH_3CHO decomposition was significant, CH_4 was formed [12]. On ceria supported Pt-Rh catalyst at low conversion also acetaldehyde was produced. Methane was detected in trace amounts at 473 K and in substantially increasing amounts by 573 K while a considerable decrease occurred in the amount of both ethanol and acetaldehyde. At this temperature a sharp increase in CO_2 and a gradual increase in H_2 concentration were observed [13]. Ru containing supported catalysts are good candidates for hydrogen formation via partial oxidation of ethanol [14] in the presence of water. Varying the steam ethanol ratio of the feed resulted in relatively small changes in conversion and selectivity, but significant effects were observed for changes in the oxygen to ethanol ratio. Supported Rh catalysts are amongst the most active samples in ethanol reforming, including oxidative steam reforming [15–21], but the oxidation of it has not been studied well yet on these samples, a detailed investigation was carried out only on Rh/ceria [22]. Among the noble metals (Rh, Ru, Pd, Pt) supported on ceria-coated alumina foams Rh showed the highest activity [23].

Rh proved to be an excellent catalyst for many reactions including steam reforming of ethanol due to its unique electronic structure and certain physico-chemical properties and in addition Rh brakes the CC bond in ethanol easier. The other important issue is the nature of the support. In this respect the acidity and reducibility factors are relevant. For example, during SRE, acidic supports like alumina (Al_2O_3) favour dehydration and thereby increase the tendency for coke formation due to the polymerization of ethylene [16,24–26]. However, on ceria (CeO_2), which is considered to be a basic support, dehydration is limited and its redox properties hinder coke formation [27,28]. Titania (TiO_2) provides easy electron transfer to the metal and from the metal back to titania [29]. Another important physico-chemical property of the oxide support is its reducibility. Reducible supports such as ceria improve catalyst stability due to their high oxygen storage capacity (OSC) and oxygen mobility. The oxygen exchange capacity of cerium oxide is associated with its ability to reversibly change oxidation states between Ce^{4+} and Ce^{3+} [30–32]. The easily accessible oxygen can react with carbon species as soon as it forms and this process keeps the metal surface free of carbon, thus inhibiting deactivation [28,33–35].

Naturally, the surface properties of both the metal and the oxide support, and also the metal/oxide interface determine the formation and stability of the intermediates present in the ethanol transformation processes. It is generally accepted that the primary step in alcohol activation is the formation of alkoxide [35]. Depending on the particular metal, dehydrogenation and CC bond scission lead to the formation of alkoxide, oxametallacycle, aldehyde, acyl and coke on the surface and mostly H_2, CH_4, CO and aldehyde in the gas phase [23,36–41].

In the present work, we aim at finding correlations between the surface properties of supported Rh catalysts (such as acid-base character, or reducibility) and their catalytic activity in ethanol oxidation. The investigation of Rh based supported catalysts in the partial oxidation of ethanol may contribute to establishing the mechanism of oxidative steam reforming of ethanol, too. The different Rh-containing catalysts are characterized by diffuse reflectance infrared Fourier transform spectroscopy (DRIFTS), X-ray photoelectron spectroscopy (XPS), and temperature programmed reduction (spectroscopy) (TPR). In the catalytic reaction of ethanol oxidation (2:1 molar ratio), the conversion of ethanol and the product distribution were studied on rhodium catalysts under the same conditions using different supports.

2. Experimental

2.1. Materials

The catalysts were prepared by impregnating the supports with the aqueous solution of $RhCl_3 \cdot 3H_2O$ salt (Johnson Matthey 99.99% metal basis) to yield a 1 wt% metal content. SiO_2 (Cab-O-Sil, 198 m^2/g), TiO_2 (Degussa P25, 50 m^2/g), Al_2O_3 (Degussa P110C1, 100 m^2/g) and CeO_2 (Alfa Aesar 75 m^2/g) were used as support. The impregnated powders were dried at 383 K and the fragments of catalyst pellets were oxidized at 473 K for 30 min and reduced at 673 K for 1 h in the catalytic reactor.

The gases used were of commercial purity. O_2 (99.995%), H_2 (99.995%) and Ar (99.996%) were used without further purification. Both ethanol (99.9% Merck HPLC quality) and triply distilled water were used after a freeze and pump purification process.

2.2. Methods

The catalytic reactions were carried out in a fixed bed continuous-flow reactor (100 mm × 10 mm o.d.). The amount of catalysts used was usually 50 mg. The dead volume of the reactor was filled with quartz chips. The C_2H_5OH/O_2 ratio in the reacting gas mixture was usually 2/1 for partial oxidation. Ethanol was introduced into an evaporator with the help of an infusion pump (Assistor PCI); the evaporator was flushed with Ar- or Ar+O_2 (flow: 80 ml/min). The space velocity is ~96 000 h^{-1} in our experiments. The composition of the carrier mixture is as follows: 7 mol% ethanol, 3.5 mol% oxygen and the rest is argon. The ethanol containing Ar flow entered the reactor through an externally heated tube avoiding condensation. Analyses of the products and reactants were performed with an Agilent 6890 N gas chromatograph using HP-PLOT/Q column. The products were detected simultaneously by TC and FI detectors.

The adsorption and temperature programmed desorption (TPD) or reaction (TPO) studies were carried out in a microbalance (Netzsch STA 409 PC) connected to a mass spectrometer (Pfeiffer QMS 200). Before the experiments the sample was oxidized and reduced at the same temperature and for the same time as mentioned above, then the chamber was flushed with He and cooled down to room-temperature. The adsorption of ethanol was performed by bubbling the carrier gas through the ethanol at 273 K for 30 minutes. The amount of adsorbed ethanol was followed by measuring the weight changes by the microbalance. After ethanol adsorption the sample was flushed again by He-flow at 300 K for 15 min, and then the catalyst was heated up with a rate of 20 K/min up to 900 K in He for the TPD or in O_2 (TPO) stream.

The infrared spectra were recorded with a BioRad FTS-135 type FTIR spectrometer, with a wave number accuracy ±2 cm^{-1}. All spectra presented are difference spectra. Experiments were carried out with a diffuse reflectance infrared cell (Spectra Tech) with CaF_2 windows, adapted to a BioRad FTS-135 type FTIR spectrometer. In one set of experiments, the interaction of ethanol with and without oxygen was studied. In another case, the interaction of the same solid with the reaction mixture was monitored at varying temperatures. The spectra were taken at different temperatures. After each temperature was reached, it was kept constant for 10 min to stabilize the sample before obtaining the spectrum. The spectrum of the sample after the reduction step was used as background.

For XPS studies, the powder samples were pressed into pellets with ca. 1 cm diameter and a few tenth of mm thickness, which were placed into the load lock of the spectrometer. Sample treatments were carried out in a high-pressure cell (catalytic chamber) connected to the analysis chamber via a gate valve. They were pre-treated in the same way as described above. After the pre-treatment, they were cooled to room temperature in flowing

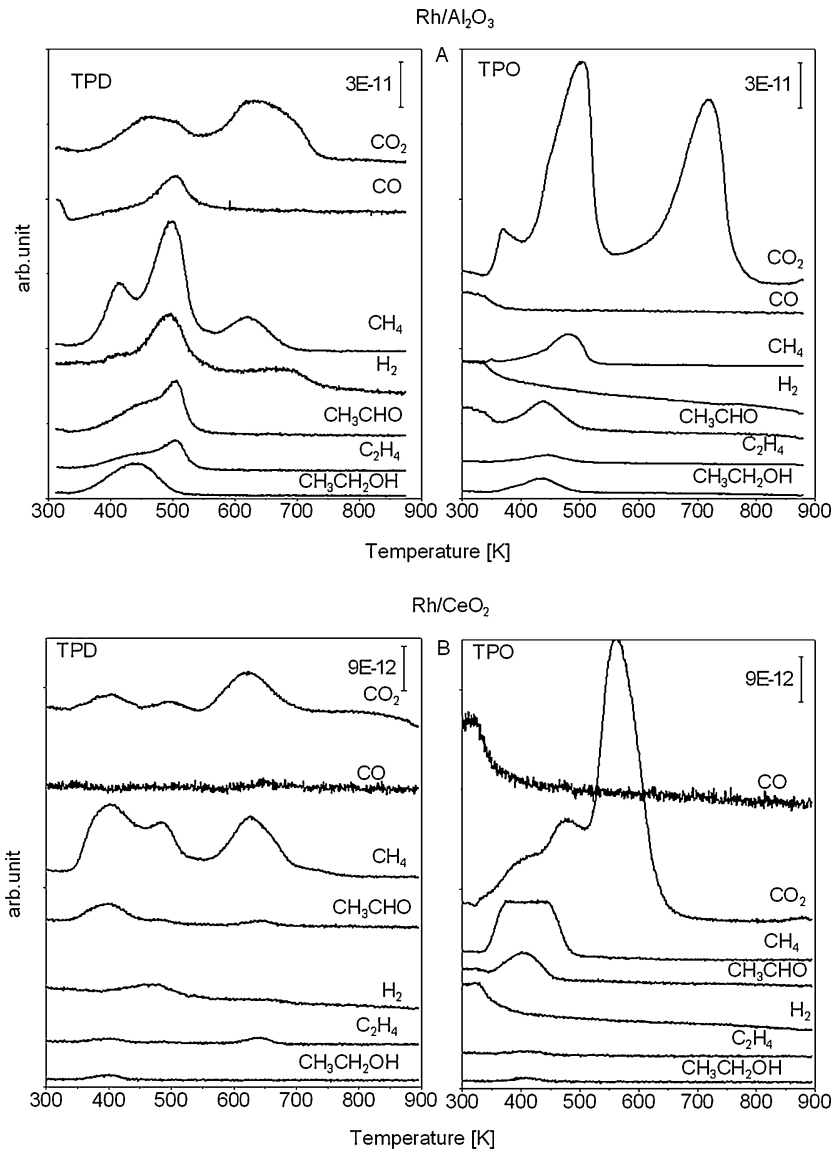

Fig. 1. Temperature programmed desorption (TPD) and temperature programmed oxidation of ethanol on 1% Rh/Al_2O_3 (A) and on 1% Rh/CeO_2 (B) catalysts.

nitrogen. Then, the high-pressure cell was evacuated; the sample was transferred to the analysis chamber in high vacuum (i.e., without contact to air), where the XP spectra were recorded. As the next step, the sample was moved back into the catalytic chamber, where it was treated with the reacting gas mixture at the reaction temperature with the same experimental conditions as used for the catalytic reaction. XP spectra were taken with a SPECS instrument equipped with a PHOIBOS 150 MCD 9 hemispherical electron energy analyzer, using Mg Kα radiation ($h\nu = 1253.6$ eV). The X-ray gun was operated at 210 W (14 kV, 15 mA). The analyzer was operated in the FAT mode, with the pass energy set to 20 eV. Typically five scans were summed to get a single spectrum. For data acquisition and evaluation both manufacturer's (SpecsLab2) and commercial (CasaXPS, Origin) software were used. A charging of several eV was experienced for all samples. The binding energy scale was corrected by fixing the Ce 3d u‴ peak (see below) to 916.8 eV, the Al 2p peak to 74.7 eV and the Si 2p peak to 103.4 eV, when using the given supports.

The dispersion of the supported Rh catalysts was determined by hydrogen adsorption assuming 1:1 stoichiometry between the metal and the H atom. The adsorption isotherms were measured in a conventional gas volumetric apparatus at room temperature, after the same pre-treatment as mentioned above. The dispersion values are as follows: for 1% Rh/Al_2O_3 29 %, for 1% Rh/SiO_2 31%, for 1% Rh/TiO_2 36% and for 1% Rh/CeO_2 38%.

3. Results and Discussion

3.1. Temperature programmed reactions (TPD and TPO)

The temperature programmed reaction spectroscopies were carried out after adsorption of ethanol at room temperature heating the sample in He (TPD) or in O_2 atmosphere (TPO) with 20 K/min. Both spectroscopies can give useful preliminary qualitative information about the surface reactions on different oxide supported Rh catalysts. In the course of our experiments we investigated the processes on all supported Rh catalysts, but only for demonstration we only present results obtained on two catalysts: one with a rather acidic (Rh/Al_2O_3) the other with a rather basic (Rh/CeO_2) support (Fig. 1A and Fig. 1B).

After C_2H_5OH adsorption on Al_2O_3 mainly C_2H_4 desorbed in TPD experiments, but small amounts of CH_3CHO, CO_2 and CH_4 were also detected. C_2H_4 appeared in a narrow peak ($T_{max} = 565$ K). CO_2 and acetaldehyde desorbed in a lower and broader temperature range,

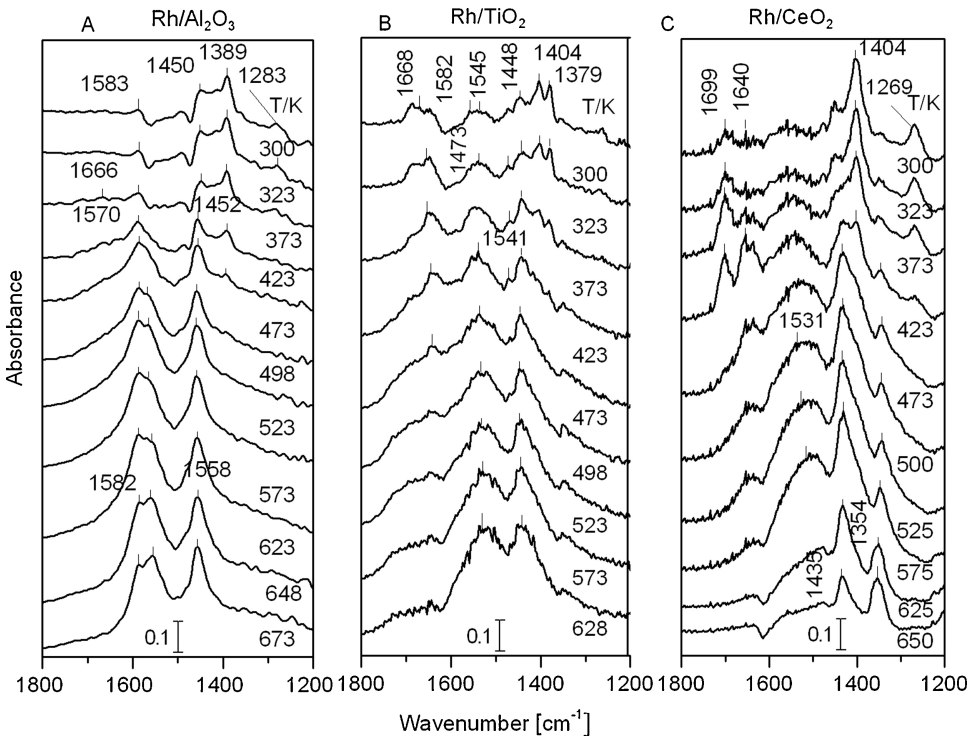

Fig. 2. Infrared spectra registered after the adsorption of ethanol on Rh/Al_2O_3 [A], on Rh/TiO_2 [B], on Rh/CeO_2 [C] and heated in oxygen flow (TPO).

at 420–570 K, where the ethanol desorption was also detected [16]. When ethanol was adsorbed on Rh/Al_2O_3 catalysts the amounts of products increased, the main components were CO_2, CH_4, CH_3CHO, H_2, and CO. Much less ethylene formed on this sample than on Al_2O_3 alone. In this case there is a high temperature desorption stage in which CO_2, CH_4 and H_2 were formed (Fig. 1A). Heating the ethanol adsorbed on Rh/Al_2O_3 in oxygen flow mainly CO_2 was detected but below 500 K a small amount of CH_4 and CH_3CHO were also observed. Above 550 K only CO_2 was detected and the TPO peak maximum was about 50 K higher than that of TPD. In the latter case the CO_2 peak has a high temperature shoulder at about 700–705 K.

When ethanol was adsorbed on SiO_2 or on Rh/SiO_2 all products desorbed up to 500 K either in He or in O_2 flow. The main products were CO_2, CH_3CHO, CH_4, C_2H_4 and C_2H_5OH with almost equal intensity. A small amount of CO_2 was detected at nearly 800 K only during the TPO of ethanol adsorbed on Rh/SiO_2.

In accordance with our earlier results [42] on TiO_2 support and on Rh/TiO_2 catalyst H_2, CO_2, CH_4, CH_3CHO and C_2H_4 formation were detected. When the adsorbed ethanol was heated in oxygen stream desorption stages were at 350-450 K, and besides of a small amount of ethanol, CO, C_2H_4, CH_3CHO, and CH_4 were formed. At higher temperature, above 600 K, CO_2 and smaller amounts of CO, CH_4, CH_3CHO and H_2 were detected in narrow peaks.

On Rh/CeO_2 catalyst, mainly CH_4 and smaller amounts of CO_2, H_2 and CH_3CHO formation were detected below 550 K, at higher temperatures, between 600-700 K CO_2, CH_4 and trace amount of C_2H_4 were formed (Fig. 1B). In contrast to a previous finding [43], CO formation was not observed in gas phase. This indicates that surface CO, which is detectable in DRIFTS (see below) interacts with ceria forming CO_2. In the presence of oxygen, significant amount of CO_2 production was observed, the main peak was detected at 600-700 K (Fig. 1B). At lower temperature some CH_4 and CH_3CHO formation were also observed. In generally we may conclude that most surface intermediates are oxidized during TPO.

DRIFTS studies give more valuable information on the adsorbed species during heat treatment. The formation of surface species in C_2H_5OH adsorption and their further reactions in the presence of oxygen were studied. Before presenting the data with oxygen, we summarize the most important IR results obtained at different temperatures in vacuum in our laboratory in harmony with the literature findings. These results were already published and generally accepted on different oxide supported Rh catalysts [16,27,36–43]. The bands observed at 300 K in the C-H stretching region (3100-2600 cm^{-1}) monotonously lost their intensities with the increase of temperature up to 573 K. Several absorption bands can be detected at 1200-1460 cm^{-1} at 300 K due to different modes of ethoxide species. These bands disappeared at 450-523 K depending on the supporting oxide. In addition, bands attributed to adsorbed acetaldehyde at 1715-1762 cm^{-1}, linear CO at 2007-2050 cm^{-1} and bridge bonded CO at 1899 cm^{-1} were detected already from room temperature. Aldehyde formation showed maximum at ~423 K. CO bands disappeared at 773 K from Rh/alumina and Rh/ceria, and at 623 K from Rh/titania. Above 373 K new bands appeared at 1575 and 1474-1468 cm^{-1} (attributed to surface acetate species), they were present up to 673-773 K.

The ethoxide species react faster in the presence of oxygen during heat treatment. The corresponding vibrations at 1200-1460 cm^{-1} and at 2860-2970 cm^{-1} disappeared on Rh/alumina, on Rh/silica at 573 K, on Rh/titania and on Rh/ceria at around 473 K. Different spectral changes were observed at 1200-1800 cm^{-1} on different oxide supported Rh samples during TPO (Fig. 2). On Rh/Al_2O_3 peaks due to acetate formation were detected at 1452 cm^{-1} and 1583 cm^{-1} already at room temperature. Their intensities increased and above 423 K the feature from the υ(OCO) vibration in acetate splitted into two peaks (1558-1582 cm^{-1}), presumably due to different orientations of acetate (Fig. 2A). The source of acetate could be the aldehyde intermediate which is produced transiently from the reaction of ethanol/ethoxide (see below reaction (6)). A small intensity peak appeared at ~1666 cm^{-1}, which was present up to 423 K. This peak was tentatively assigned to adsorbed water, which formed during OH assisted ethoxide formation. The formation of adsorbed water was supposed during ethanol

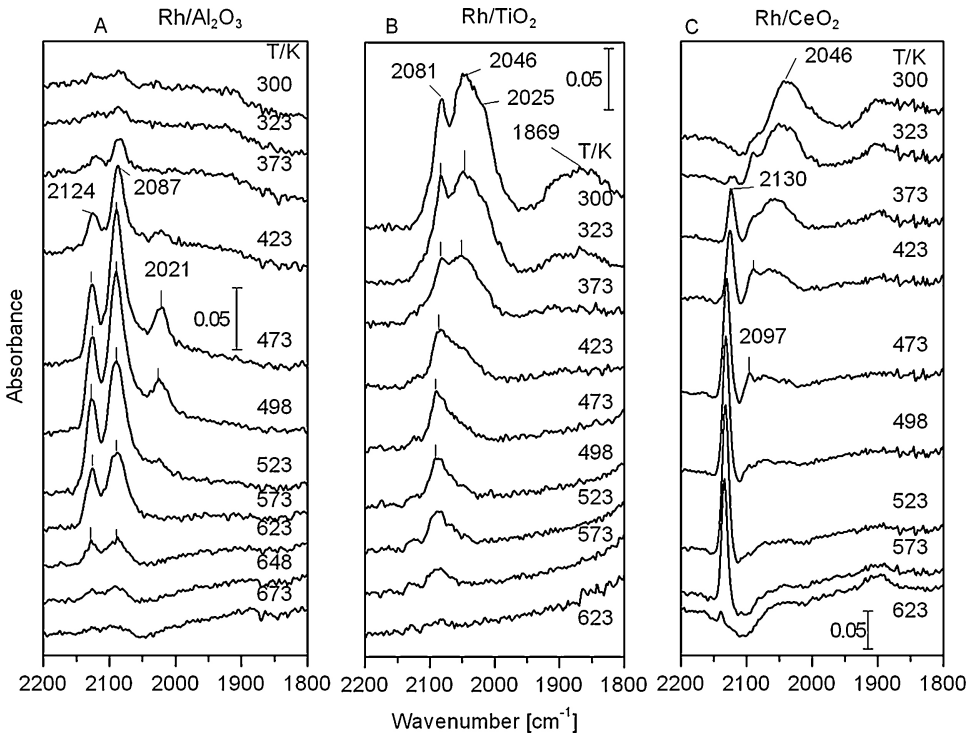

Fig. 3. Infrared spectra registered in adsorbed CO regime, after the adsorption of ethanol on Rh/Al_2O_3 [A], on Rh/TiO_2 [B], on Rh/CeO_2 [C] and heated in oxygen flow (TPO).

transformation reactions on many oxide supported metal surfaces [8,17] and in several oxidation reactions.

$$C_2H_5OH + OH_{(a)} \rightarrow C_2H_5O_{(a)} + H_2O_{(a)} \quad (5)$$

More complex spectral features were observed on Rh/TiO_2. After oxygen introduction to the ethanol covered surface at 300 K several infrared bands were detected in the range of 1200-1800 cm^{-1} (Fig. 2B): 1379, 1404, 1448, 1473, 1545, 1582 and 1668 cm^{-1}. The thermal stability of the bands at 1404 and 1473 cm^{-1} ($\delta_{as}(CH_3)$, $\delta_s(CH_3)$ in ethoxide) changed parallel with other ethoxide bands. They disappeared between 450-475 K. Interestingly, a relatively strong band developed at 1668 cm^{-1} which was present even at 500-523 K and can be attributed to the formation of adsorbed HCOOH. The band at 1670 cm^{-1} was observed earlier on TiO_2 and TiO_2(110) after the adsorption of formic acid [44,45]. A similar band was detected during the adsorption of HCOOH on Rh/TiO_2 at 300 K [46]. The formation of HCOOH in the present case may easily be explained by the reaction of transiently formed acetaldehyde with oxygen:

$$C_2H_5OH_{(a)} \rightarrow C_2H_4O_{(a)} + 2H_{(a)} \quad (6)$$

$$C_2H_4O_{(a)} + 2O_a \rightarrow HCOH + HCOOH_{(a)} \quad (7)$$

Adsorbed formic acid was present in our TPO experiments up to 500-523 K. Besides the appearance of adsorbed HCOOH, IR bands were observed at 1379 and 1582 cm^{-1} which can be identified as adsorbed formate ($HCOO_a$) which forms via the decomposition of adsorbed HCOOH [46]:

$$HCOOH_{(a)} \rightarrow HCOO_{(a)} + H_{(a)} \quad (8)$$

$$2H_{(a)} + O_{(a)} \rightarrow H_2O_{(a)} \quad (9)$$

Adsorbed formate and its further reactions were found during ethanol transformation on Rh/TiO_2, too [42]. The infrared bands at 1448 and 1541–1545 cm^{-1} appeared already at 323 K due to the formation of acetate, in harmony with literature data [16–18,27]. The transiently formed aldehyde can readily react with oxygen forming surface acetate (CH_3COO):

$$CH_3CHO_{(a)} + 2O_{(at)} \rightarrow CH_3COO_{(a)} + OH_{(a)} \quad (10)$$

The acetate group was present up to 673 K (Fig. 2). Earlier acetate formation was observed directly during the thermal reaction of acetaldehyde on Rh/Al_2O_3 and Rh/TiO_2 [47,48].

In the next part we investigate the reaction of adsorbed ethanol in the presence of oxygen on Rh/CeO_2. Up to 473 K some ethoxide bands (1354, 1404 cm^{-1}) were detected. The 1269 cm^{-1} band observed at 300 K was attributed to the δ(OH) mode of molecularly adsorbed ethanol and was detectable up to 473 K. Molecular ethanol was previously also detected on Ir/Al_2O_3 [16], on Pd/CeO_2 [28] and on Co/CeO_2 [17]. Similarly to the alumina supported catalyst adsorbed water may also be present around 1666 cm^{-1}. In addition, a band of *ή – adsorbedacetaldehyde*, υ(C=O) at 1699 cm^{-1} was observed even at room temperature. Its intensity increased up to 423 K and then suddenly disappeared. Acetate bands (1435, 1531 cm^{-1}) developed already from ~350 K (see reaction step (10)). It is very remarkable that above 323 K a band developed due to acetyl species at 1640 cm^{-1}. This intermediate was detected during partial oxidation on this catalyst [22]. This species could be the possible precursor of acetate formation:

$$CH_3CHO_{(a)} \rightarrow CH_3CO_{(a)} + H_{(a)} \quad (11)$$

When the temperature was increased above 600 K, two peaks were dominant: at 1354 cm^{-1} and 1435 cm^{-1} which can be attributed to carbonate [49]. It is important to note that in contrast to the titania support case, no formic acid and formate ($CHOO_a$) species were detected.

The oxidation reaction over supported Rh is particularly adapted for infrared study because CO adsorbs on supported Rh in several well-characterized states [50–53]. From the monitoring of DRIFT spectra in the interaction of adsorbed ethanol with oxygen during heat treatment (TPO) in the frequency range of CO (1800-

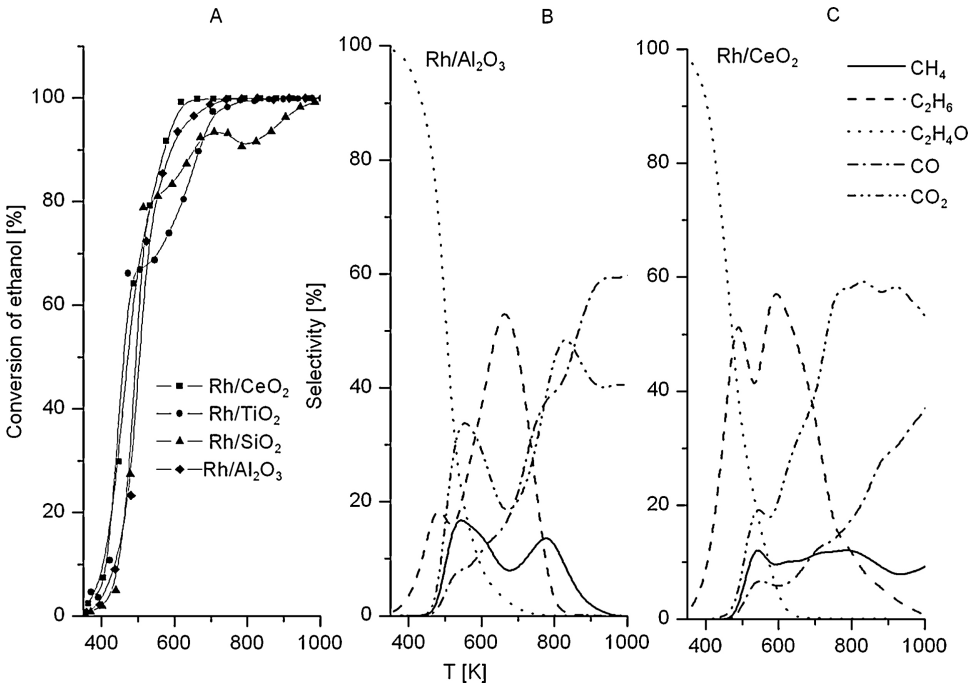

Fig. 4. Conversion of ethanol vs. temperature on supported Rh samples [A] and the selectivity of product formation as a function of temperature on Rh/Al_2O_3 [B] and on Rh/CeO_2 [C] during heating up (2 K/min) the sample in the ethanol-oxygen flow.

2200 cm^{-1}), we may get information about the adsorption mode of CO, and from the oxidation state and morphology of Rh, too.

On Rh/Al_2O_3 near room temperature only a very small peak was observed at 2087 cm^{-1}. Between 423 and 523 K, three bands of adsorbed CO were detected (Fig. 3). The band at 2087 cm^{-1} intensified; two new peaks were developed at 2124 and 2021 cm^{-1} with different intensities. After the assignment published in the literature, the peak at 2124 cm^{-1}, which exists up to 648 K, can be attributed to Rh^{3+} oxidation state [51,53]. The peak at 2087 cm^{-1} can be rendered to separate Rh^{+} particles and in addition it may contribute to the spectral feature due to the formation of gem dicarbonyl species together with the band at 2021 cm^{-1}. From this spectral feature we may conclude that Rh is in 3+ and 1+ oxidation states, presumably with high dispersion.

On Rh/TiO_2 catalyst we did not detect peak due to Rh^{3+}. At 300 K three bands were observed. The peak at 2046 cm^{-1} can be ordered to the linearly bonded CO on Rh^0. This peak disappeared above 473 K. The pair of bands at 2081 and 2025 cm^{-1} can be attributed partially to the gem dicarbonyl species containing symmetric and antisymmetric stretching modes of CO bonded to isolated Rh^{+} sites [50–52]. Upon heating the lowest frequency peak disappeared at 373 K. The peak at 2081 cm^{-1} bonded to partially oxidized Rh disappeared only above 573 K (Fig. 3).

On Rh/CeO_2 the spectral feature was different. First the linearly bonded CO appeared. This peak disappeared at ~473 K. A sharp peak developed above 323 K at 2130 cm^{-1}. This is from CO bonded to Rh^{3+} sites and it disappeared at 623 K. Between 423 K-498 K a weak feature appeared at 2097 cm^{-1}. In this temperature range Rh is mainly in Rh^{+} oxidation state.

3.2. *The partial oxidation of ethanol over Rh-based catalysts using different supports*

In the first series of the measurements the partial oxidation of ethanol (ethanol/oxygen ratio was 2:1) was studied by gradually heating the catalysts in the reacting gas mixture from 323 K (Fig. 4A). The ethanol conversion started to increase slightly above 373 K in the case of Rh/CeO_2 and Rh/TiO_2. The 50% of ethanol conversion was achieved about 473 K on these samples. This conversion was measured roughly at about 500 K on Rh/Al_2O_3 and on Rh/SiO_2. On 1% Rh/CeO_2 the ethanol was completely missing from the outlet gas mixture above 620 K. 100% conversion was obtained about 30 K higher temperatures on Rh/Al_2O_3. A local minimum was observed in the conversion of ethanol above 550 K in the case of Rh/TiO_2 and Rh/SiO_2 (Fig. 4A). The possible reason is that these catalysts, in spite of the presence of O_2, may significantly promote the reaction of aldehyde with hydrogen which forms in many reaction steps in this high temperature regime (for example 2,3).

$$CH_3CHO_{(a)} + 2H_{(a)} \rightarrow CH_3CH_2OH_{(g)} \quad (12)$$

On all catalysts acetaldehyde was the dominant product at low temperatures. With increasing temperature CH_4, C_2H_6, CO, CO_2 and water were formed. Hydrogen, which forms in many reaction paths, can be predominantly oxidized below 1000 K and at the applied relatively high flow rate (80 ml/min). Reduction of the total flow rate increased the syngas selectivity and decreased the higher products [23]. Detailed product distributions obtained on Rh/Al_2O_3 and on Rh/CeO_2 are displayed in Fig. 4B and 4C. Similar features were observed on Rh/TiO_2 and on Rh/SiO_2.

Detailed catalytic studies were performed at 493 K where the conversion was relatively low. The conversion dependence on reaction time is displayed on different supported Rh catalysts in Fig. 5A. In general, the conversion of ethanol increased significantly at the beginning and then, after 60-120 min, following a slow decrease, the activity remained constant. At this constant reaction temperature the selectivity changed different ways on different supports. On Rh/Al_2O_3 almost only acetaldehyde was detected in the first 50 min. After its selectivity dropped to 27% and the formation of CO_2 and CH_4 started to increase and reached a constant value. CO production remained below 2% (Fig. 5B). On Rh/SiO_2 also acetaldehyde formed first, after reaching a minimum its selectivity slowly increased. The CO_2 selectivity change was the opposite. The selectivity of methane showed a constant value (~20%) after 20 min. On Rh/TiO_2 the main products were acetaldehyde and CO_2, their

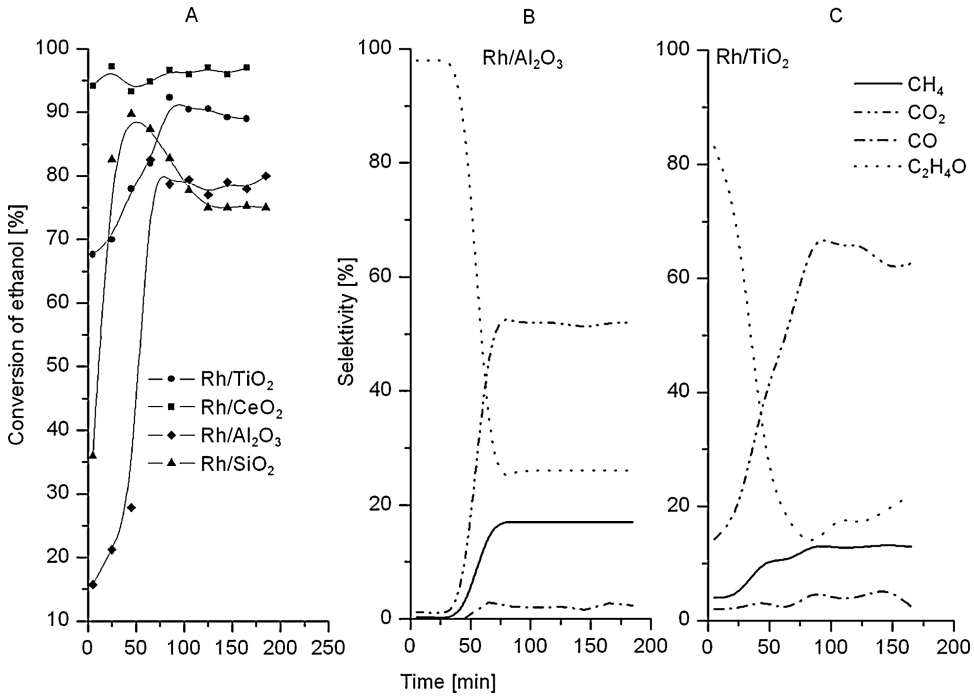

Fig. 5. Conversion of ethanol on different oxides used as supports [A] and the products selectivity on Rh/Al_2O_3 [B] and on Rh/TiO_2 [C] at 493 K in the oxidation of ethanol.

Table 1
Some characteristic data for ethanol oxidation at 493 K on the supports and on different supported Rh catalysts at 150th min reaction time.

	Conversion %	Selectivity %			
		CH_3CHO	CO_2	CO	CH_4
1% Rh/Al_2O_3	79	27.3	52.9	2.3	17.5
Al_2O_3	13	97	–	0.3	–
1% Rh/SiO_2	75	17.3	62	1.7	19
SiO_2	0.7	95	1	3	0.8
1% Rh/TiO_2	90	22	62.6	2.4	13
TiO_2	15.7	99	–	0.3	0.4
1% Rh/CeO_2	97	13.8	77.9	6.4	1.9
CeO_2	17	98	0.8	0.2	0.3

amounts changed in the opposite way, acetaldehyde decreased, CO_2 increased with time. Less amount of CH_4 and CO were detected (Fig. 5C). On Rh/CeO_2 the CO_2 formation was the highest (75%), its value remained constant in time. Acetaldehyde formed at the beginning with ~20% selectivity, than rapidly decreased, the methane formation showed a maximum, after 100 min its value remained constant. A small amount of ethylene, acetone were also detected. Some characteristic data for ethanol oxidation at 493 K on different supported Rh catalysts are collected in Table 1. This table contains the conversion and selectivity data obtained on pure oxide supports, too.

3.3. *Oxidation state of Rh after ethanol-O_2 reaction at 493 K: an XPS study*

The Rh oxidation state was studied by XPS on different supports after the partial oxidation of ethanol at 493 K. Prior to reaction, the supported Rh was reduced at 673 K in all cases. The dispersion values for 1% Rh catalysts and the IR data of adsorbed CO showed that Rh is in a rather well-dispersed state on Al_2O_3, TiO_2 and on CeO_2 supports. This binding energy difference can be attributed to the small particle size of Rh clusters due to the final state effect in XPS [54–56]. Basically, we may also consider another reason for the upward shift of the Rh 3d peaks. One explanation could be an electronic interaction between Rh and the reducible oxide, which was observed between reduced titania and ceria and different metals including Rh[17,57–60]. The presence of a high number of defects and oxygen vacancies in ceria or in titania could initiate an increased electron flow between the metal and the support.

Accordingly the Rh 3d photoemission signals appeared at somewhat higher binding energies as was observed on bulk phase metallic rhodium. On Rh/Al_2O_3 the Rh $3d_{5/2}$ peak was detected at 308.2 eV, after ethanol oxidation (at 10 min reaction time) it moved to higher binding energy and could be fitted with two peaks at 309.8 and 308.2 eV indicating that during the reaction Rh is in partially oxidized state (Fig. 6A). The intensity of the peak at 309.8 eV increased a little bit after 70 min reaction time. Two C 1s XPS signals were detected after reaction (Fig. 6B). The C 1s peak from carbonyl like species was detected at 285.9 eV mainly due to the formation of adsorbed CO (see DRIFTS measurements below). The 289.3 eV peak is attributed to acetate [61]. Carbon signals disappeared after flashing the catalysts to 600 K (not shown).

The Rh $3d_{3/2}$ component on the SiO_2 support was at located at 307.1 eV after reduction at 673 K, indicating the presence of higher crystallite sizes. The Rh 3d signal has significantly lower intensity compared to the Al_2O_3 and CeO_2 supported samples, indicating the lack of extended available metal surface. It is interesting that in the case of Rh/SiO_2 the Rh $3d_{3/2}$ peak remained in the same position after ethanol oxidation at 493 K. Besides some broadening, the peak was detected at 307.1 eV even after 70 min reaction time (Fig. 6C). The structure of the carbon XP spectrum was also different from the Rh/Al_2O_3 case (Fig. 6D). The peak appeared at 285.0 eV, which may represent C-C and C-H bonds. The photoemission at 286.9 eV is assigned to the methyl end of chemisorbed acetaldehyde [62]. Carbon-free surface was obtained after oxygen treatment at 600 K.

Due to the high dispersion of Rh on ceria, the Rh $3d_{3/2}$ signal appeared at 307.6 eV after reduction. When the ethanol-oxygen mixture was introduced, after 10 and mainly 70 min a small peak was detected at 309.6 eV corresponding to the oxidation of Rh on this support, too (Fig. 7A). Some spectral changes were also observed on the ceria support after reaction. The exact characterization of Ce compounds by X-ray photoelectron spectroscopy is

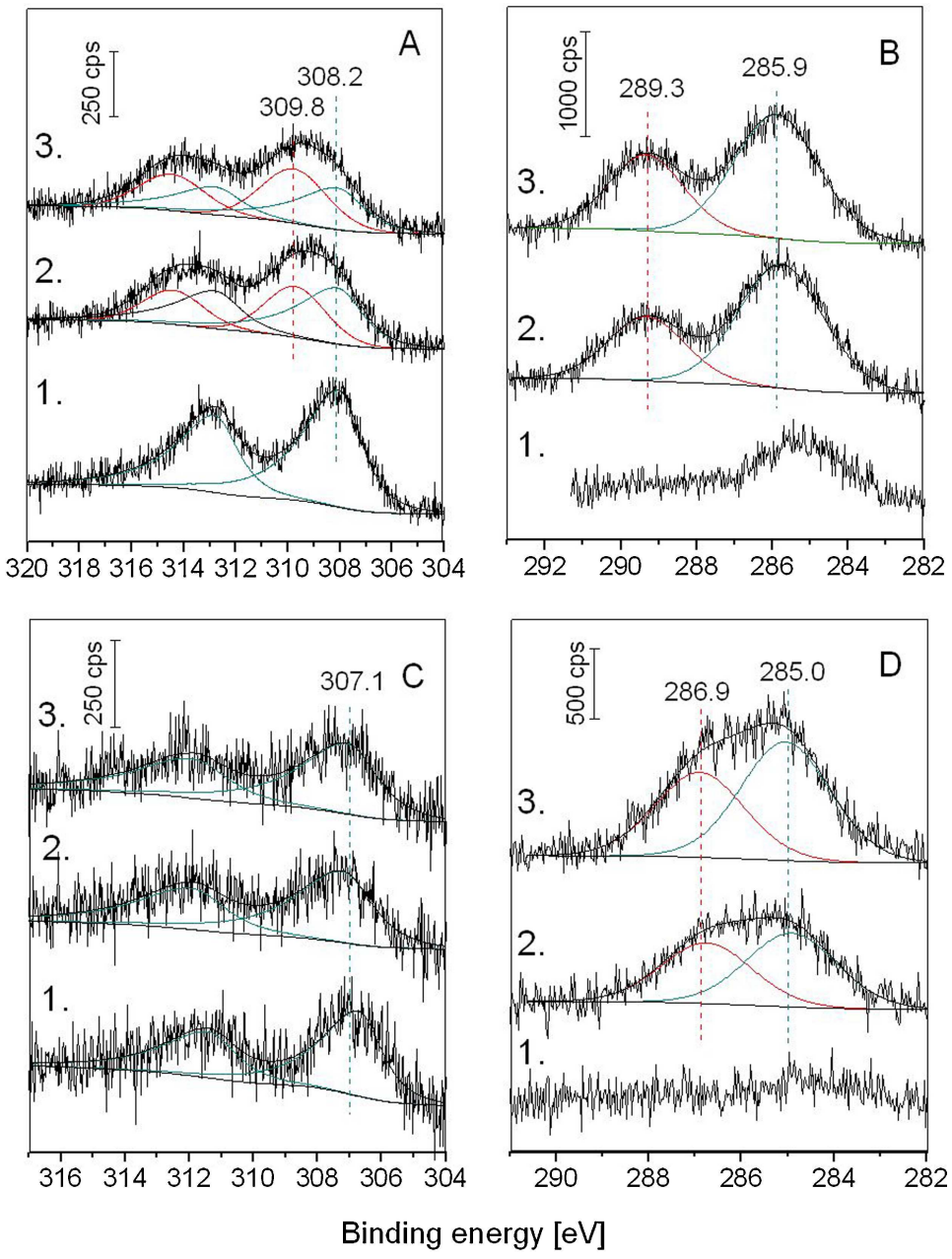

Fig. 6. Rh 3d (A) and C 1s (B) XP spectra obtained on Rh/Al_2O_3 after reduction (1) after 10 min (2) and 70 min (3) reaction time in ethanol oxidation at 493 K. Rh 3d (C) and C 1s (D) XP spectra obtained on Rh/SiO_2 after reduction (1) after 10 min (2) and 70 min (3) reaction time in ethanol oxidation at 493 K.

a challenge because of the complex nature of the Ce 3d spectrum. The 3d spin-orbit doublet can split up into maximum ten individual peaks when both Ce^{3+} and Ce^{4+} species are present on the surface. The shake-up and possibly shake-down features reflect the interaction between the valence band of the ligands and the Ce 4f orbital [17,18,41,63–65]. After the reduction of ceria at 600 K a new feature appeared on the Ce 3d spectrum at 903.4 and 885.7 eV corresponding to Ce^{3+} (Fig. 7B1). These features became stronger after 10 and 70 min treatment in the ethanol-oxygen mixture at 493 K (Fig. 7B2 and 7B3), but it was significantly less intense than after ethanol adsorption alone at this temperature (Fig. 7B4). It means that the reaction mixture led to the partial oxidation of Rh and to a certain re-oxidation (but not full) of ceria. As regards the C 1s signal after reaction we could detect two intense peaks at 285.0 and 286.9 eV (Fig. 7C). The former can be attributed to some CH species while the second one may correspond to acetaldehyde species, which was also detectable in DRIFTS (see below).

3.4. In situ DRIFTS experiments during ethanol-O_2 reaction at 493 K

During the DRIFTS measurements we monitored the IR bands during the partial oxidation of ethanol at 493 K on different oxide supported Rh catalysts.

After the introduction of the $C_2H_5OH + O_2$ mixture at 493 K to the Rh/Al_2O_3 catalyst a negative spectral feature at 3720 cm^{-1} was detected that refers to the interaction of ethanol with the OH groups of the support. Bands in the 2972-2880 cm^{-1} regime can be assigned as the C-H stretching vibration of adsorbed ethoxide. Ethoxide related bands are also detectable at around 1049 cm^{-1}. In the first minute of the reaction bands at 1580-1597, 1460-1470 and 1331 cm^{-1} appeared on the spectra which can be attributed to the acetate species. The intensities of these absorbances increased in time (Fig. 8A). Interestingly, a shoulder appeared at the high frequency side at 1631 cm^{-1}, very probably due to the formation

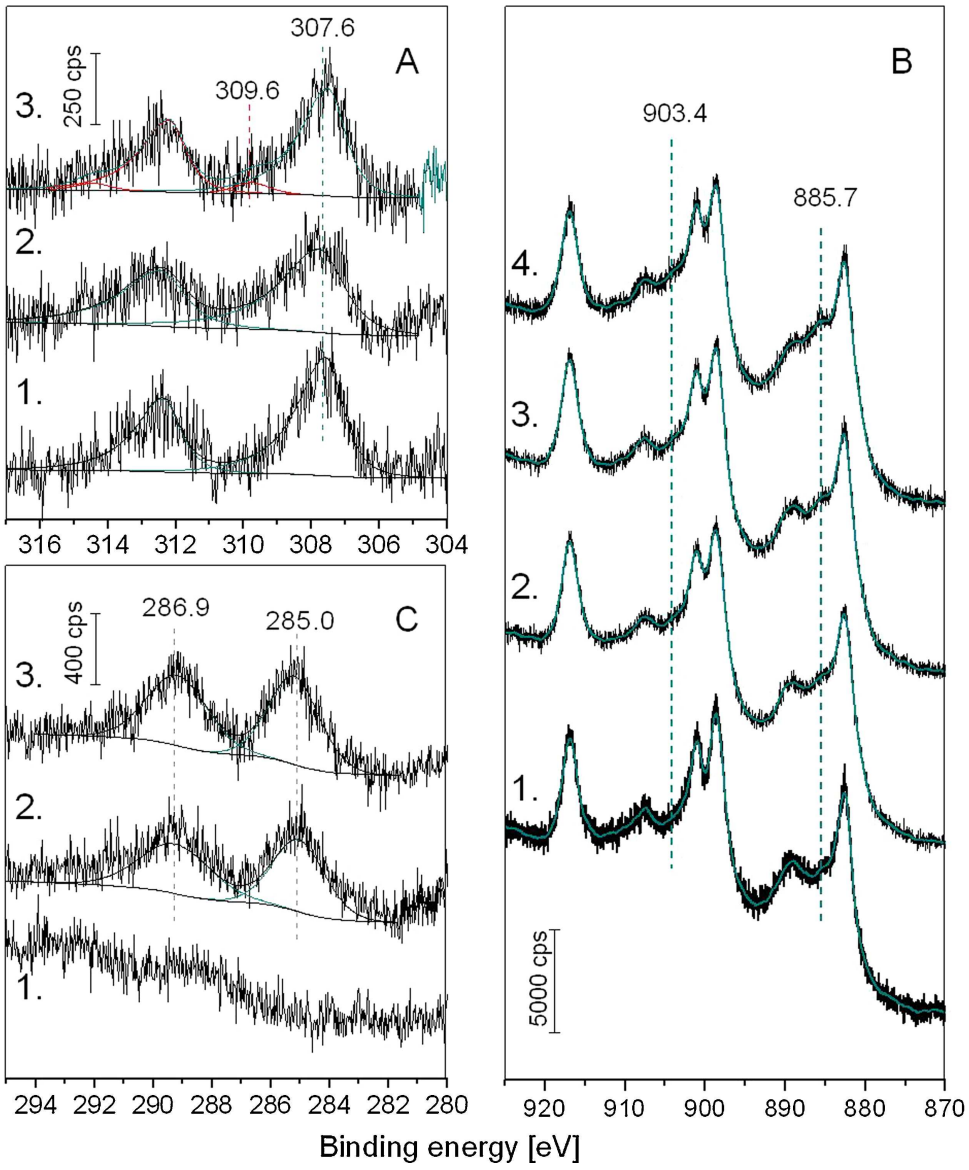

Fig. 7. Rh 3d XP spectra obtained on Rh/CeO_2 after reduction (1) after 10 min (2) and 70 min (3) reaction time of ethanol oxidation at 493 K [A]. Ce 3d spectra obtained on Rh/CeO_2 [B] after reduction (1) after 10 min (2) and 70 min (3) reaction time of ethanol oxidation and ethanol adsorption (4) at 493 K. C 1s spectra obtained on Rh/CeO_2 [C] after reduction (1) after 10 min (2) and 70 min (3) reaction time in ethanol oxidation at 493 K.

of acetyl species which was observed on the Rh/CeO_2 catalyst in the reaction of adsorbed ethanol during heating in O_2 atmosphere (reaction 11).

In the CO region bands at 2119, 2086 and 2018 cm^{-1} were detected. The intensities of these bands first increased but after 15 minutes of the reaction a significant decay was observed. On the spectra registered after 45 minutes the band at 2119 cm^{-1} was missing. As was discussed above, the peak at 2119 cm^{-1}, which exists up to 30 min reaction time, can be attributed to Rh^{3+} oxidation state [51,53]. The peak at 2086 cm^{-1} can be assigned to the separate Rh^+ particles and in addition it may also represent the formation of gem dicarbonyl species together with the band at 2012 cm^{-1}. This finding is also supported by the XPS results (Fig. 6A), the rhodium is in partially oxidized state during the reaction. The gas phase formation (band at 2360 cm^{-1}) can be attributed to the oxidation of CO and acetaldehyde and to the decomposition of acetate. CH_4 formation is explained also by the decomposition of acetate. Aldehyde is very unstable on Rh/Al_2O_3, it readily oxidized to acetate or left the surface (see Fig. 5B).

The IR spectra taken during ethanol oxidation on Rh/SiO_2 were simpler (Fig. 8B). The band of OH groups changed in the same way as on Rh/Al_2O_3. Some bands below 1450 cm^{-1} and at 2850-2983 cm^{-1} indicate the presence of ethoxide species during reaction. Adsorbed CO and acetate formation was not observed on this silica supported Rh catalyst. A relatively strong aldehyde group is present at 1749-1731 cm^{-1}. The gas phase CO_2 (2360 cm^{-1}) can be attributed to the direct reaction of acetaldehyde with O_2 (12).

$$CH_3CHO_{(a)} + 5O_{(a)} \rightarrow 2CO_2 + 2H_2O \quad (12)$$

In the case of Rh/TiO_2 the most intense bands due to acetate were observed at 1439 and 1539 cm^{-1}. A very weak band of adsorbed CO was measured at 2080 cm^{-1}. An intense band at 1724 cm^{-1} from adsorbed acetaldehyde was detected (Fig. 9A). Very probably the end products: CO_2, CO and CH_4 were produced via the oxidation of acetaldehyde through acetate intermediate.

A very similar picture was observed in the case of Rh/CeO_2 catalyst. Ethoxide bands were registered during the reaction. The OH consumption was not remarkable in contrast to other supported

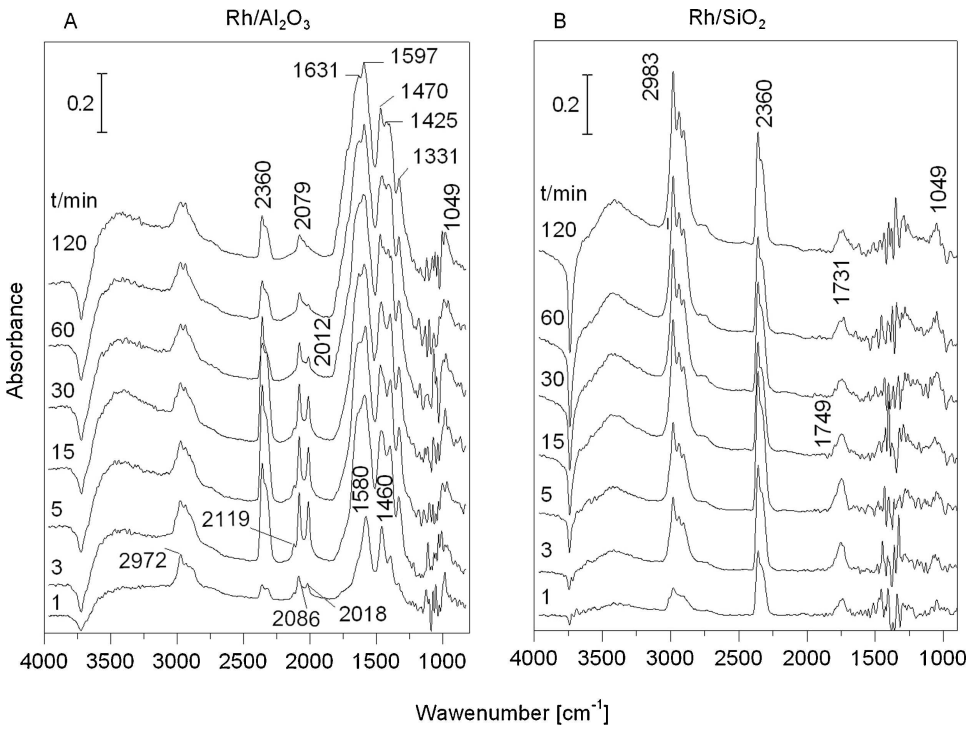

Fig. 8. In situ infrared spectra registered during ethanol oxidation on Rh/Al_2O_3 [A] and Rh/TiO_2 [B] at 493 K.

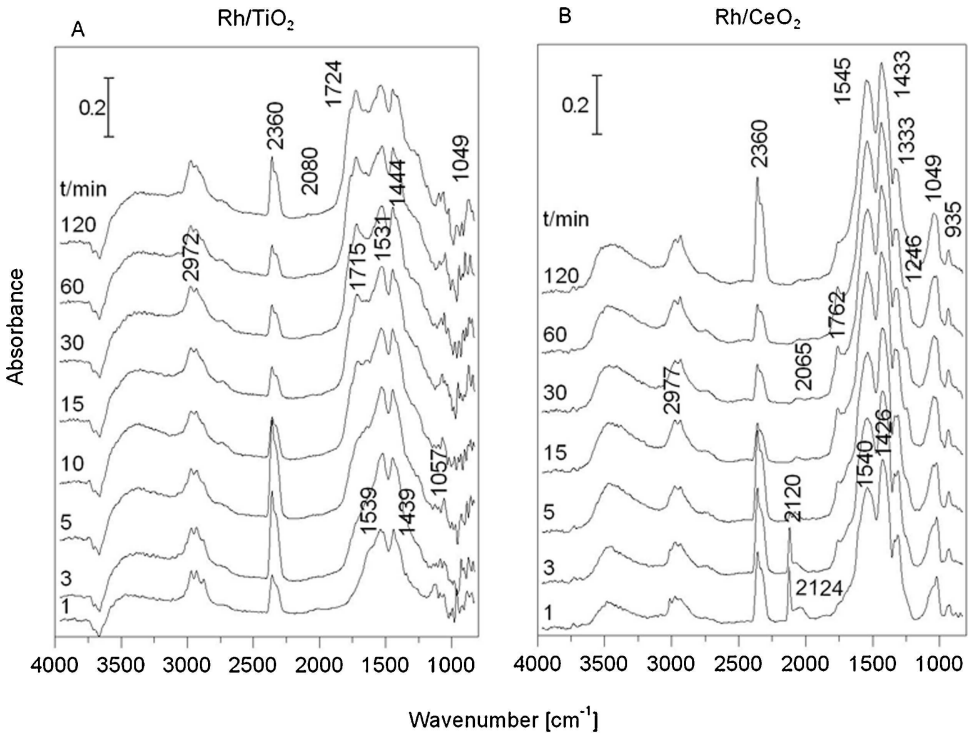

Fig. 9. In situ infrared spectra registered during ethanol oxidation on Rh/TiO_2 [A] and Rh/CeO_2 [B] at 493 K.

Rh cases. At the beginning of the reaction a strong band of CO bonded to oxidized Rh was detected at 2124 cm^{-1}, with increasing the reaction time only linearly adsorbed CO bonded to metallic Rh was observed. Acetate bands (1333, 1433 and 1545 cm^{-1}) were present at this reaction temperature. A strong peak from adsorbed aldehyde appeared at 1762 cm^{-1}. This feature was observed previously at this temperature on the same Rh/CeO_2 catalyst [22]. The authors detected adsorbed acetyl species at 1638 cm^{-1} at much lower temperature (at 300-373 K). The acetyl species can be oxidized to acetate or can be decomposed, forming CH_4, H_2 and CO. A sharp peaking at 3020 cm^{-1} indicates gas phase methane formation.

The *ή – adsorbedacetaldehyde*, υ(C=O) at 1699 cm^{-1} was observed in the reaction of adsorbed ethanol with oxygen even at room temperature. Its intensity increased up to 423 K and then suddenly disappeared during TPO (Fig. 2C). A more stable aldehyde

(at 1762 cm^{-1}) formed during the ethanol-oxygen reaction at 473-573 K (in present work and ref. [20]). This acetaldehyde adsorbed on the Lewis sites through one of the oxygen lone pairs (more stable species) can be the source of higher temperature acetaldehyde formation and desorption. For Rh-based catalysts, the ethoxide species lost one H atom from the terminal methyl group and then adsorbed in a cyclic configuration (oxametallacycle intermediate) [36]. This intermediate was more stable on Rh than $\acute{\eta}^2$(C,O) and $\acute{\eta}^1$(O) configurations of acetaldehyde and decomposed at higher temperatures, producing CO, CH_x and C_x, which were oxidized to CO_2. We cannot rule out this pathway in our work, the bands corresponding to oxametallacycle intermediate below 1000 cm^{-1} could not be detected due to the poor resolution of DRIFTS spectrum and to CaF_2 windows applied in this region. Moreover, the bands associated to the five-membered ring oxametallacycle species above 1000 cm^{-1} are similar to the bands related to ethoxide species and could not be distinguished from them.

4. Conclusion

The main aim of our study is to investigate the effect of oxide support on the product distribution and the stability of transiently formed intermediates in ethanol partial oxidation on Rh catalysts. Combined gas chromatographic (GC), X-ray photoelectron spectroscopic (XPS) and in-situ diffuse reflectance Fourier-transform infrared spectroscopy (DRIFTS) experiments were carried out. The highest conversion was obtained on ceria supported Rh at 493 K. XPS and DRIFTS studies revealed that Rh is in partially oxidized states on alumina, titania and ceria. In spite of the presence of O_2, CeO_2 is not fully oxidized during the partial oxidation of ethanol. The aldehyde surface species from ethoxide plays a key role in the formation of reaction products. Its decomposition/oxidation leads to the production of acetate which decomposes to CO_2, CO and CH_4. The acetaldehyde species are oxidized to acetate or dehydrogenated to acetyl species or may desorb on Rh/Al_2O_3 and on Rh/CeO_2. Furthermore, the acetate species previously formed can be decompose to CH_4, CO and/or oxidized to CO_2 via carbonate species at higher temperature depending on the oxide support. The ethoxide species may also dehydrogenated by H elimination from the terminal methyl group generating cyclic intermediate (oxametallacycle compound) and decomposes at high temperature. On Rh/TiO_2 catalyst the other important intermediate is $HCOOH/HCOO_{(a)}$ formed via aldehyde oxidation. This form is stable up to 450 K. On silica support acetaldehyde was the dominant intermediate.

Acknowledgements

The financial support by the Alexander von Humboldt Foundation within the Research Group Linkage Programme is acknowledged. This research was also partially funded by TÁMOP-4.2.4.A/2-11/1-2012-0001 —by the European Union and by the European Social Fund.

References

[1] T.B. Reed, R.M. Lerner, Science 28 (1973) 1299.
[2] E. Gauthier, B. Benzinger, Electrochim. Acta 128 (2014) 238.
[3] M.G. Coleman, A.M. Brown, B.A. Bolton, H.R. Guan, Adv. Synth. Catal. 352 (2010) 967.
[4] Y. Wang, J. Sung, J. Appl. Catal. 4 (2014) 1078.
[5] L. Jelemensky, B.F.M. Kunster, G.B. Marin, Catal. Lett. 30 (1995) 269.
[6] R.D. Gonzalez, M. Nagai, Appl. Catal. 18 (1985) 57.
[7] P. Gallezot, Catal. Today 37 (1997) 405.
[8] L.V. Mattos, B.H. Jacobs, F.B. Noronha, Chem. Rev. 112 (2012) 4094, and references therein.
[9] A. Sapi, F. Liu, X. Cai, C.M. Thompson, H. Wang, K. An, J.M. Krier, G.A. Somorjai, Nano Lett. 14 (2014) 6727.
[10] R.D. Gonzalez, M. Nagai, Appl. Catal. 18 (1985) 57.
[11] L.V. Mattos, F.B. Noronha, J. Power Sources 152 (2005) 50.
[12] L.V. Mattos, F.B. Noronha, J. Catal. 233 (2005) 45.
[13] P.-Y. Sheng, A. Yee, G.A. Bowmaker, H. Idriss, J. Catal. 208 (2002) 393.
[14] D.K. Liguras, K. Goundani, X.E. Verykios, Int. J. Hydrogen Energy 29 (2004) 419.
[15] C. Diagne, H. Idriss, A. Kiennemann, Catal. Commun. 3 (2002) 565.
[16] A. Erdőhelyi, J. Raskó, T. Kecskés, M. Tóth, M. Dömök, K. Baán, Catal. Today 116 (2006) 367.
[17] Zs. Ferencz, A. Erdőhelyi, K. Baán, A. Oszkó, L. Óvári, Z. Kónya, C. Papp, H.-P. Steinrück, J. Kiss, ACS Catal. 4 (2014) 1205.
[18] E. Varga, Zs. Ferencz, A. Oszkó, A. Erdőhelyi, J. Kiss, J. Mol. Catal. A 397 (2015) 127.
[19] F. Frusteri, S. Freni, V. Chiodo, S. Donaato, G. Bonura, S. Cavallaro, Int. J. Hydrogen Energy 31 (2006) 2190–2193.
[20] E. Vasseli, G. Comellei, R. Rosei, S. Frusteri, S. Cavallaro, Appl. Catal. A 281 (2005) 139–147.
[21] X. Han, Y. Yu, H. He, W. Shan, Int. J. Hydrogen Energy 38 (2013) 10293–10304.
[22] A.M. Silva, L.O.O. Costa, A.P.M.G. Barandas, L.E.P. Borges, L.V. Mattos, F.B. Noronha, Catal. Today 133-135 (2008) 755–761.
[23] J.R. Salge, G.A. Deluga, L.D. Schmidt, J. Catal. 235 (2005) 69–78.
[24] M. Badlani, I.E. Wachs, Catal. Lett. 75 (2001) 137–149.
[25] D. Kulkarni, I.E. Wachs, Appl. Catal., A 237 (2002) 121–137.
[26] J. Raskó, M. Dömök, K. Baán, A. Erdőhelyi, Appl. Catal. A: General 299 (2006) 202.
[27] L.V. Mattos, B.H. Jacobs, F.B. Noronha, Chem. Rev. 112 (2012) 4094–4123.
[28] A. Yee, S.J. Morrison, H.J. Idriss, J. Catal. 186 (1999) 279–295.
[29] U. Diebold, Surf. Sci. Rep. 48 (2003) 53 (and references therein).
[30] J. Kaspar, P. Fornasiero, M. Graziani, Catal. Today 50 (1999) 285–298.
[31] A. Trovarelli, In Catalysis by Ceria and Related Materials, Imperial College Press, London, 2002, pp. p. 1–58.
[32] M. Happel, J. Myslivecek, V. Johánek, F. Dvorak, O. Stetsovych, Y. Lykhach, V. Matolín, J. Libuda, J. Catal. 289 (2012) 118–126.
[33] H. Song, U.S. Ozkan, J. Catal. 261 (2009) 66–74.
[34] A.M. da Silva, K.R. de Souza, L.V. Mattos, G. Jacobs, B.H. Davis, F.B. Noronha, Catal. Today 164 (2011) 234–239.
[35] E. Martono, J.V. Vohs, ACS Catal. 1 (2011) 1414–1420.
[36] M. Mavrikakis, M. Barteau, J. Mol. Catal. A 131 (1998) 135–147.
[37] C. Diagne, H. Idriss, A. Kiennemann, Catal. Commun. 3 (2002) 565–571.
[38] M. Tóth, M. Dömök, J. Raskó, A. Hancz, A. Erdőhelyi, Chem. Eng. Trans. 4 (2004) 229–234.
[39] J. Raskó, M. Dömök, K. Baán, A. Erdőhelyi, Appl. Catal., A 299 (2006) 202–211.
[40] J. Raskó, J. Kiss, J. Appl. Catal. A 287 (2005) 252–260.
[41] L. Óvári, S. Krick Calderon, Y. Lykhach, J. Libuda, A. Erdőhelyi, C. Papp, J. Kiss, H.-P. Steinrück, J. Catal. 307 (2013) 132–139.
[42] J. Raskó, A. Hancz, A. Erdőhelyi, Appl. Catal. A: General 269 (2004) 13.
[43] A. Yee, S.J. Morrison, H. Idriss, Catal. Today 63 (2000) 327–335.
[44] M.A. Henderson, J. Phys. Chem. B 101 (1997) 221–229.
[45] L.F. Liao, W.C. Wu, C.Y. Chen, J.L. Lin, J. Phys. Chem. B 105 (2001) 7678–7685.
[46] T. Kecskés, J. Raskó, J. Kiss, Appl. Catal. A: General 268 (2004).
[47] J. Raskó, J. Kiss, Catal. Lett. 101 (2005) 71–77.
[48] J. Raskó, T. Kecskés, J. Kiss, Appl. Catal. A: General 287 (2005) 244–251.
[49] G.N. Vayssilov, M. Mihaylov, P. St Petkov, K.I. Hadjiivanov, K.M. Neyman, J. Phys. Chem. C 115 (2011) 23435–23454.
[50] J.T. Yates, T.M. Duncas, S.D. Worley, R.W. Vaughan, J. Chem. Phys. 70 (1979) 1219.
[51] C.A. Rice, S.D. Worley, C.W. Curtis, J.A. Guin, A.R. Tarrare, J. Chem. Phys. 74 (1981) 6487.
[52] F. Solymosi, M. Pásztor, J. Phys. Chem. 89 (1985) 4789.
[53] C.H. Dai, S.D. Worley, Chem. Phys. Lett. 114 (1995) 286–290.
[54] M.G. Mason, Phys. Rev. B 27 (1983) 748.
[55] W.F. Egelhoff Jr., Surf. Sci. Rep. 6 (1986) 253 (and references therein).
[56] L. Óvári, J. Kiss, Appl. Surf. Sci. 252 (2006) 8624–8629.
[57] F. Solymosi, Catal. Rev. 1 (1968) 233–255.
[58] M.A. Vannice, R.L. Garten, J. Catal. 56 (1979) 236–248.
[59] F. Solymosi, A. Erdőhelyi, T. Bánsági, J. Catal. 68 (1981) 371–382.
[60] G. Pótári, D. Madarász, L. Nagy, B. László, A. Sápi, A. Oszkó, Á. Kukovecz, A. Erdőhelyi, Z. Kónya, J. Kiss, Langmuir 29 (2013) 3061–3072.
[61] D.R. Mullins, S.D. Senanayake, T.-L. Chen, J. Phys. Chem. C 114 (2010) 17112–17119.
[62] T.-L. Chen, D.R. Mullins, J. Phys. Chem. C 115 (2011) 3385–3392.
[63] G. Praline, B.E. Koel, R.L. Hance, H.I. Lee, J.M. White, J. Electron Spectr. and Related Phenom. 21 (1980) 17–30.
[64] A. Pfau, K.D. Schierbaum, Surf. Sci. 321 (1994) 71–80.
[65] C.J. Nelin, P.S. Bagus, E.S. Ilton, S.A. Chambers, H. Kuhlenbeck, H.-J. Freund, J. Quant. Chem. 110 (2010) 2752–2764.